Effect of interfacial thermal resistance and nanolayer on estimates of effective thermal conductivity of nanofluids

(Article begins on next page)

04 August 2020
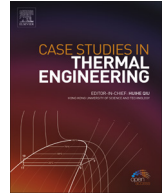
Effect of interfacial thermal resistance and nanolayer on estimates of effective thermal conductivity of nanofluids

Ali Khodayari[a], Matteo Fasano[a], Masoud Bozorg Bigdeli[b], Shahin Mohammadnejad[a], Eliodoro Chiavazzo[a], Pietro Asinari[a],*

[a] Energy Department, Politecnico di Torino, Corso Duca degli Abruzzi 24, Torino 10129, Italy
[b] Department of Mechanical Engineering, University of Alberta, Edmonton, Canada T6G 2G8

A B S T R A C T

Colloidal suspensions of nanoparticles (nanofluids) are materials of interest for thermal engineering, because their heat transfer properties are typically enhanced as compared to the base fluid one. Effective medium theory provides popular models for estimating the overall thermal conductivity of nanofluids based on their composition. In this article, the accuracy of models based on the Bruggeman approximation is assessed. The sensitivity of these models to nanoscale interfacial phenomena, such as interfacial thermal resistance (Kapitza resistance) and fluid ordering around nanoparticles (nanolayer), is considered for a case study consisting of alumina nanoparticles suspended in water. While no significant differences are noticed for various thermal conductivity profiles in the nanolayer, a good agreement with experiments is observed with Kapitza resistance $\approx 10^{-9}\,\mathrm{m^2K/W}$ and sub-nanometer nanolayer thickness. These results confirm the classical nature of thermal conduction in nanofluids and highlight that future studies should rather focus on a better quantification of Kapitza resistance at nanoparticle-fluid interfaces, in order to allow bottom up estimates of their effective thermal conductivity.

1. Introduction

Since the first report on their peculiar thermal conductivity in 1995, thermophysical properties of colloidal suspensions of nanoparticles (nanofluids) have been widely investigated in the biomedical and engineering fields [1].

In the biomedical sector, nanofluids show applications in cancer therapy, drug delivery, imaging and sensing [2,3]. As far as engineering applications are concerned, nanofluids can be employed in mechanical systems as lubricants or magnetic sealants, in structural systems as magneto-rheological fluid dampers, in automotive or electric systems as coolants (including evaporators and condensers) [4–11], and in energy systems for either direct or indirect solar thermal energy absorption [12–17].

In particular, suspending thermally conductive nanoparticles in conventional fluids with the aim of improving their heat transfer properties has been among the most investigated and controversial research areas [18–20]. Researchers have studied experimental, semi-empirical and theoretical models for the thermal conductivity of nanofluids, which is typically enhanced respect to the base fluid one [21–25]. While the classical nature of thermal conduction in nanofluids forces their thermal conductivities to fall between lower and upper Maxwell bounds for homogeneous systems [26], a general model accommodating the numerous experimental evidences has been under debate for more than two decades. In particular, classic Effective Medium Theories (EMTs), such as Maxwell-Garnett (MG) [27] or Bruggeman (BR) [28] approximations, have been progressively amended to include the nanoscale

---

* Corresponding author.
  E-mail address: pietro.asinari@polito.it (P. Asinari).

effects at nanoparticle-fluid interface, as well as the nanoparticle size, shape and aggregation [13].

In this work, we analyze two nanoscale phenomena involved in the effective thermal conductivity of nanofluids, namely interfacial thermal resistance (Kapitza resistance) and fluid ordering around nanoparticles (nanolayer). The sensitivity of BR approximation to these interfacial effects is systematically evaluated. Results show that Kapitza resistance plays a significant role in determining the effective thermal conductivity of nanofluids; whereas, the approximation employed for the thermal conductivity profile within the nanolayer has not a sensible effect. Moreover, the influence of nanolayer on the effective thermal conductivity appears as negligible if realistic values of nanolayer thickness are considered, namely less than 1 nm. This analysis suggests that future studies on thermal properties of nanofluids should focus on a better quantification of Kapitza resistance at the nanoparticle-fluid interface.

2. Methods

Several models based on EMT have been proposed to predict the thermal conductivity of nanofluids. In particular, Bruggeman approximation predicts the effective thermal conductivity of homogeneous suspensions as:

$$\phi\left(\frac{\lambda_p - \lambda_{eff}}{\lambda_p + 2\lambda_{eff}}\right) + (1 - \phi)\left(\frac{\lambda_f - \lambda_{eff}}{\lambda_f + 2\lambda_{eff}}\right) = 0, \tag{1}$$

where ϕ is the particle volume fraction, while λ_p, λ_f and λ_{eff} are the particle, base fluid, and effective thermal conductivity of nanofluid, respectively. The Bruggeman approximation is particularly suitable for nanosuspensions with unbiased configuration, namely a mix of linearly aggregated and well-dispersed nanoparticles [26]. Note that, for low volume concentrations, MG and BR models lead to approximately equal predictions. Models based on EMT have demonstrated good accuracy with experiments for a large span of particle volume fractions: for example, the benchmark study on the thermal conductivity of nanofluids carried out by Buongiorno et al. found a good agreement (i.e. < 20% mismatch) in the range ϕ= 0.001–3% [29].

2.1. Nanolayer

The nanolayer is a structured layer of fluid molecules at the interface with nanoparticle surface, and it generally shows properties different from the bulk fluid ones [30–32]. In particular, in case of hydrophilic nanoparticles immersed in aqueous media, the average thermal conductivity of nanolayer ($\overline{\lambda}_l$) has reportedly higher values respect to the base fluid one (see Fig. 1) [33]. The nanolayer typically shows sub-nanometer thickness, namely a few layers of water molecules in the proximity of nanoparticle surface [34,35].

Several models have been proposed to capture the effect of nanolayer on the thermal conductivity of nanofluids. For example, the EMT model modified by Yu and Choi accounts for the effect of liquid layering on the thermal conductivity of nanofluids [36]. In this model, nanoparticle (radius: r_p) and the surrounding nanolayer (thickness: t) are treated as a single particle with an equivalent radius equal to $r_p + t$. The resulting equivalent volume concentration (ϕ_e) is thus evaluated as

$$\phi_e = \phi(1 + \delta)^3, \tag{2}$$

where $\delta = \frac{t}{r_p}$ is the ratio between nanolayer thickness and particle radius. The thermal conductivity of equivalent particles (λ_{pe}) is subsequently derived from effective medium theory as

$$\lambda_{pe} = \frac{[2(1 - \gamma) + (1 + \delta)^3(1 + 2\gamma)]\gamma}{-(1 - \gamma) + (1 + \delta)^3(1 + 2\gamma)}\lambda_p, \tag{3}$$
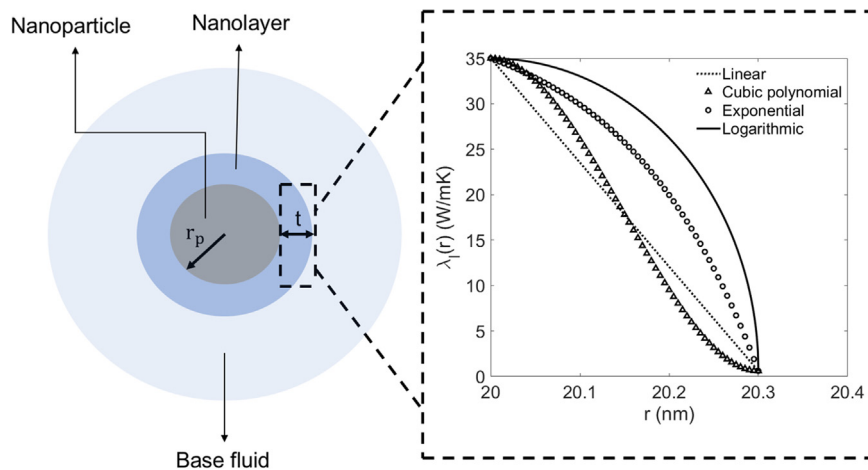

Fig. 1. Thermal conductivity profile in the water nanolayer in proximity of an alumina nanoparticle ($\lambda_f = 0.60$ W/m K, $\lambda_p = 35$ W/m K [29], $r_p = 20$ nm and $t = 0.30$ nm [30,26]). The thermal conductivity profiles in the nanolayer predicted by Eqs. (6)–(9) are compared.

being $\gamma = \frac{\bar{\lambda}_l}{\lambda_p}$. The BR model in Eq. (1) can be then modified as

$$\phi(1+\delta)^3\left(\frac{\lambda_{pe}-\lambda_{eff}}{\lambda_{pe}+2\lambda_{eff}}\right) + [1-\phi(1+\delta)^3]\left(\frac{\lambda_f-\lambda_{eff}}{\lambda_f+2\lambda_{eff}}\right) = 0. \tag{4}$$

Since the average thermal conductivity of nanolayer should present values higher than base fluid one and possibly lower than that of the particle ($\lambda_p \geq \bar{\lambda}_l \geq \lambda_f$), a continuous thermal conductivity profile ($\lambda_l(r)$) has been typically hypothesized within the nanolayer ($r_p \leq r \leq r_p + t$) [37], and $\bar{\lambda}_l$ computed as

$$\bar{\lambda}_l = \frac{t}{r_p\left(r_p+t\right)\int_{r_p}^{r_p+t}\left(\frac{1}{r^2\lambda_l(r)}\right)dr}. \tag{5}$$

Different thermal conductivity profiles in the nanolayer have been proposed in the literature. For instance, Xie et al. [37] investigated the effect of a linear $\lambda_l(r)$ profile, namely

$$\lambda_l(r) = \lambda_p - \left(\lambda_p - \lambda_f\right)\frac{r - r_p}{t}. \tag{6}$$

Jiang et al. [38], instead, introduced a cubic polynomial model for the nanolayer thermal conductivity:

$$\lambda_l(r) = \frac{(\lambda_p - \lambda_f)}{4}\left[\left(\frac{2(r-r_p)}{t}-1\right)^3 - 3\left(\frac{2(r-r_p)}{t}-1\right)\right] + \frac{\lambda_p + \lambda_f}{2}; \tag{7}$$

whereas, Kotia et al. [39] a logarithmic one

$$\lambda_l(r) = \lambda_f + \frac{\lambda_p - \lambda_f}{t}\sqrt{t^2 - (r-r_p)^2}. \tag{8}$$

Finally, Pasrija et al. [40] proposed an exponential profile for $\lambda_l(r)$, that is

$$\lambda_l(r) = \lambda_p + \left(\frac{\lambda_f - \lambda_p}{1 - e^m}\right)\left[1 - e^{\frac{m(r-r_p)}{t}}\right], \tag{9}$$

where m is a real positive value ($m = 2$ [40]). Considering Eqs. (6)–(9), Fig. 1 compares the different thermal conductivity profiles in a representative case study, which is made of an alumina nanoparticle immersed in water and surrounded by water nanolayer.

2.2. Kapitza resistance

The Kapitza resistance at nanoparticle-fluid interface also influences the effective thermal conductivity of nanofluids [41,42]. Such interfacial thermal resistance arises from the phonon scattering due to acoustic mismatch at the interface of dissimilar materials (e.g. solid-liquid phases). Kapitza resistance can be expressed as

$$R_k = \frac{\Delta T}{q}, \tag{10}$$

where ΔT is the temperature jump at the interface generated by a specific heat flux q.

To take into account this additional resistance to heat transfer in nanoparticle suspensions, the thermal conductivity of nanoparticles can be modified as

$$\lambda_p^* = \frac{2r_p}{R_k + \frac{2r_p}{\lambda_p}}, \tag{11}$$

where R_k refers to the nanoparticle-fluid interface [43]. The thermal conductivity of equivalent particles (λ_{pe}, Eq. (3)) can be then computed using λ_p^* instead of λ_p; finally, BR model (Eq. (4)) can be adopted to estimate λ_{eff}.

3. Results and discussions

3.1. Sensitivity of thermal conductivity to nanolayer and Kapitza resistance

The sensitivity of EMT-based thermal conductivity models to nanolayer thermal conductivity and Kapitza resistance has been then assessed (see Table 1 for a detailed list of tested models). A water-alumina nanofluid has been considered as a case study ($r_p = 20$ nm, $\lambda_p = 35$ W/m K, $\lambda_f = 0.60$ W/m K [29]).

On the one hand, the influence of different $\lambda(r)$ profiles on λ_{eff} is shown in Fig. 2a. As generally predicted by EMT approximations, effective thermal conductivity increases with nanoparticle volume fraction. In accordance with experimental and numerical studies in the literature [26,30], the nanolayer thickness is first taken as $t = 0.30$ nm (black lines and symbols). Results show that the models

Table 1
Models for estimating the effective thermal conductivity of nanofluids that are considered in the sensitivity analysis.

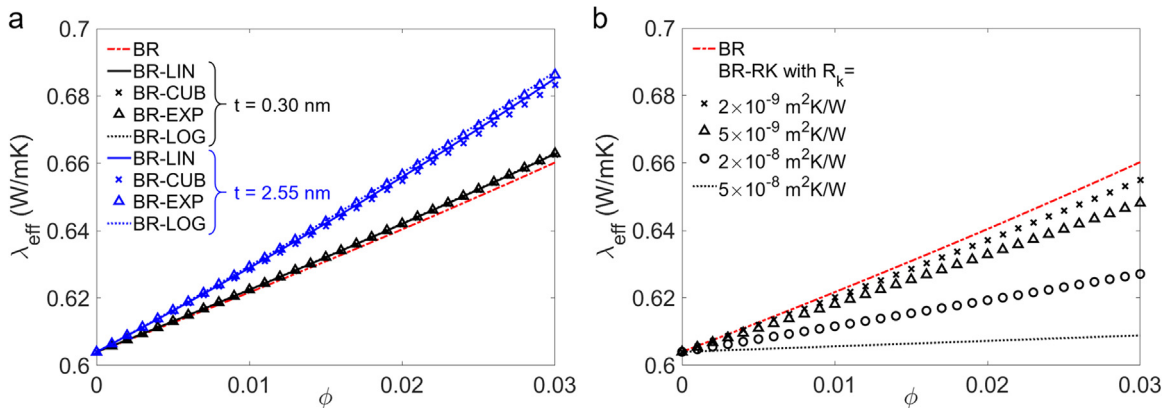| Model	λ_{eff}	$\lambda_l(r)$	Particle λ
BR	Eq. (1)	–	λ_p
BR-LIN	Eq. (4)	Eq. (6)	λ_p
BR-CUB	Eq. (4)	Eq. (7)	λ_p
BR-LOG	Eq. (4)	Eq. (8)	λ_p
BR-EXP	Eq. (4)	Eq. (9)	λ_p
BR-LIN-RK	Eq. (4)	Eq. (6)	λ_p^*, Eq. (11)

Fig. 2. Sensitivity analysis of the effective thermal conductivity with respect to (a) nanolayer thermal conductivity profile and (b) Kapitza resistance. The reported models are defined according to Table 1 and refer to alumina-water nanofluid.

accounting for nanolayer effect lead to slightly higher λ_{eff} predictions respect to BR model, namely up to 0.5% more. This is due to the fact that, while BR model considers a bulk value of thermal conductivity in the nanolayer ($\overline{\lambda}_l = \lambda_f = 0.60$ W/m K), $\overline{\lambda}_l$ is estimated as 8.54, 4.84, 13.42, and 23.21 W/m K in the BR-LIN, BR-CUB, BR-EXP, and BR-LOG models, respectively. Nevertheless, λ_{eff} predictions are substantially similar (less than 0.1% differences) among the four $\lambda_l(r)$ profiles. Blue lines and symbols in Fig. 2a, instead, represent λ_{eff} predictions obtained with the nanolayer thickness hypothesized by Tso et al. for aqueous alumina nanosuspensions with 5 nm $\leq r_p \leq 30$ nm, namely $t = 2.55$ nm [44]. Under such assumption, λ_{eff} appears to be significantly enhanced by nanolayer effect (up to 4.1% increase), while no relevant discrepancies between the different $\lambda_l(r)$ profiles are still observable (less than 0.6% differences). However, nanolayer thicknesses larger than 1 nm are at variance with consolidated experimental and numerical evidences [26].

On the other hand, Fig. 2b illustrates a general decrease of λ_{eff} with Kapitza resistance. In fact, by exploring typical values of Kapitza resistance at the interface between hydrophilic solid surfaces and water ($0.2 \times 10^{-8} - 5.0 \times 10^{-8}$ m^{2}K/W [45,46]), a sensible drop (as much as -7.8% respect to BR model) in λ_{eff} could be observed with increasing R_k.

Table 2
Experimental studies of alumina-water nanofluids that have been considered for validating the EMT-based models. Note that only experiments carried out at around room temperature (20 °C to 25 °C) are considered in this work.

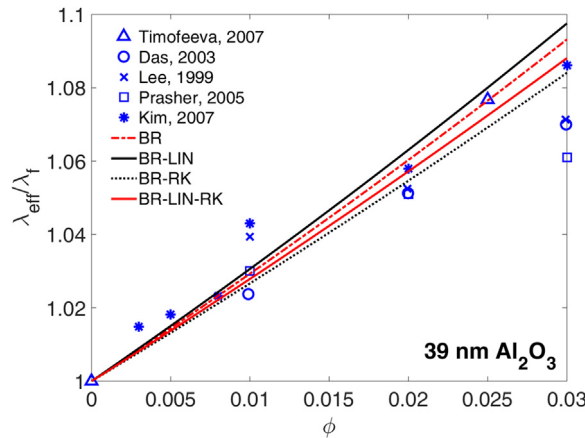| Reference	Particle diameter (nm)
Timofeeva et al. [45]	11, 40
Das et al. [47]	38.4
Lee et al. [48]	38.4
Patel et al. [49]	11, 45, 150
Beck et al. [50]	12, 46
Beck et al. [51]	12
Yiamsawasd et al. [52]	120
Chandrasekar et al. [53]	43
Prasher et al. [54]	38.4
Kim et al. [55]	38

Fig. 3. Comparison between modeling (lines) and experimental (dots) values of normalized effective thermal conductivity of nanofluids made of water and alumina nanoparticles (39 nm diameter). The reported models are defined according to Table 1; whereas, experimental data are extracted from the references in Table 2.

3.2. Experimental validation of EMT models

Experimental data from the literature are then used to assess the accuracy of effective thermal conductivity predictions by EMT-based models [45,47–55]. The detailed list of considered experimental data is given in Table 2. As a first approximation, $t = 0.30$ nm [26,30] and $R_k = 0.2 \times 10^{-8}$ m^{2}K/W (fitting value adopted in Ref. [45]) are taken as nanolayer thickness and Kapitza resistance at the alumina-water interface, respectively. Nanofluids with nanoparticles characterized by a diameter approximately equal to 39 nm are initially considered. In Fig. 3, a large mismatch with experiments is shown by the model accounting only for nanolayer effect (BR-LIN, $R^2 = 0.61$) and by the classic Bruggeman model (BR, $R^2 = 0.71$); whereas, better agreement with experiments is achieved by both the model including Kapitza resistance together with nanolayer effect (BR-LIN-RK, $R^2 = 0.80$) and the model including only the effect of Kapitza resistance (BR-RK, $R^2 = 0.84$). Note that the variability of results between different experimental sets may be due to the presence of various surfactants in the nanofluids, since surfactants strongly regulate the particle aggregation behavior and thus the resulting λ_{eff} [56].

3.3. Optimal nanolayer thickness and Kapitza resistance

Since both interfacial thermal resistance [57–59] and nanolayer [30,60,61] at the nanoscale interface between solid and liquid phase have been widely observed by experiments and simulations, the BR-LIN-RK model should - in principle - best represent the heat transfer mechanisms determining λ_{eff}. Therefore, the significant discrepancy between BR-LIN-RK model and experiments in Fig. 3 may be due to sub-optimal estimations of R_k, t or both. The sensitivity analysis reported in Fig. 4 indeed shows that, with proper
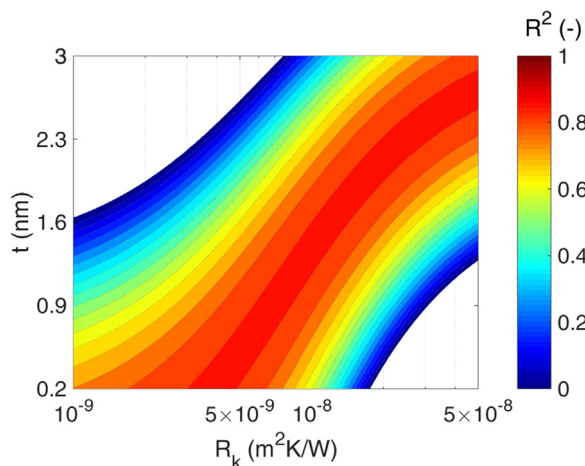

Fig. 4. Coefficient of determination (R^2) of BR-LIN-RK model fitting to the experimental results reported in Fig. 3, with different values of Kapitza resistance (R_k) and nanolayer thickness (t) at the alumina-water interface. For the sake of clarity, combinations of R_k and t leading to $R^2 < 0$ are colored in white.
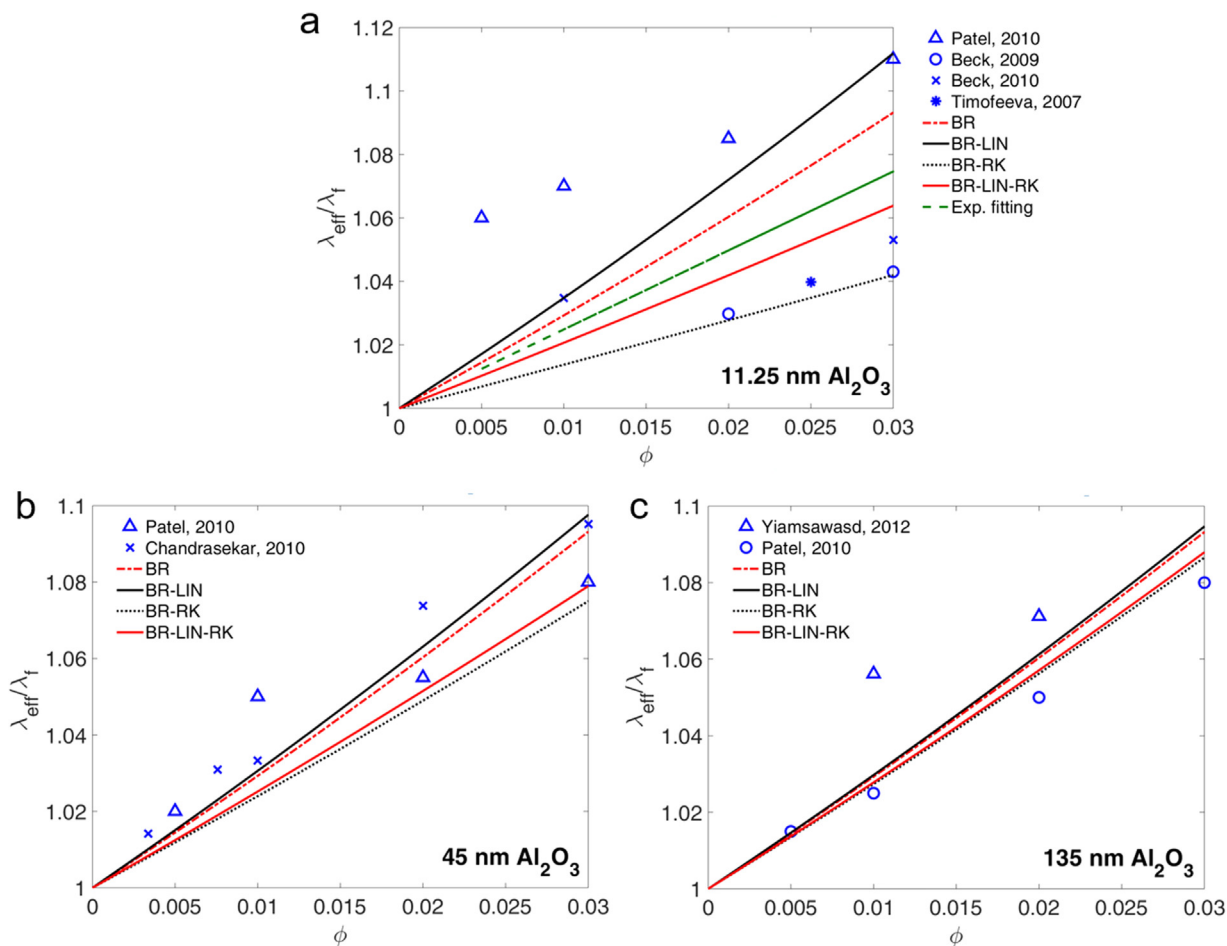
Fig. 5. Comparison between modeling (lines) and experimental (dots) values of thermal conductivity enhancement for nanofluids made of water and alumina nanoparticles with different diameters: (a) 11.25 nm; (b) 45 nm; (c) 135 nm. Models are defined according to Table 1; experimental data are extracted from the references in Table 2. Note that the dashed green line in panel (a) is a linear fitting of the reported experimental results.

combinations of R_k and t values, the BR-LIN-RK model could potentially achieve an accurate match (up to $R^2 = 0.87$) of the experimental results in Fig. 3. For example, a large coefficient of determination ($R^2 = 0.86$) is observed with $R_k = 5.0 \times 10^{-9}$ m²K/W and $t = 0.35$ nm, namely typical values of Kapitza resistance [59,62] and nanolayer thickness [30] observed in case of other metal oxide-water interfaces under fully hydrated conditions.

The latter values are then employed to evaluate the applicability of these EMT-based models with other nanoparticles sizes. Results in Fig. 5 illustrate that a better match between experiments and models is generally observed with larger particles (Figs. 5b and c), while a higher variability can be noticed with the smaller ones (Fig. 5a). In the latter case, the nanolayer extension becomes comparable with nanoparticle diameter, therefore determining an increased influence of interfacial phenomena on λ_{eff}; hence, small variations in the value of nanolayer thickness or Kapitza resistance may cause a large scattering of results. Nonetheless, the linear fitting (i.e. the average value) of experimental results in Fig. 5a presents a difference less than 0.8% with respect to the BR-LIN-RK model.

Hence, models based on effective medium theory that account for nanoscale thermal transport phenomena (interfacial thermal resistance and nanolayer) have the potential to provide good approximations of the effective thermal conductivity of suspensions of nanoparticles with a broad range of diameters. However, further researches should be devoted to measure, both numerically and experimentally, more accurate values of Kapitza resistance and nanolayer thickness at typical solid-liquid interfaces of engineering interests, for instance alumina-water ones or any other pair of interest.

4. Conclusions

Enhanced physical properties of nanofluids have led to their widespread exploitation in different fields, for instance the energy, mechanical, automotive, and biomedical ones. In particular, the thermal conductivity of such nanoparticle suspensions is generally improved respect to the base fluid one. However, nanoscale characteristics and the resulting macroscopic properties have to be better

understood to achieve a more rational design of nanosuspensions.

In this study, different models based on Bruggeman approximation have been compared with experimental data from the literature, in order to assess the sensitivity of the effective thermal conductivity of nanofluids to Kapitza resistance and liquid layering at the nanoparticle-fluid interface. First, it has been shown that estimates of effective thermal conductivity of nanofluids significantly depend on the Kapitza resistance at their solid-liquid interface. Second, results show that different hypotheses of thermal conductivity profile in the nanolayer have no significant effect on the predicted effective thermal conductivity. Third, the effective thermal conductivity is only very slightly affected by the enhanced thermal conductivity of nanolayer, at least when realistic sub-nanometer thicknesses of nanolayer are considered. In fact, the assumption of thicker water layering around nanoparticles leads to overestimated values of effective thermal conductivity.

In conclusion, EMT models accounting for nanoscale effects at the nanoparticle-fluid interface can provide good approximations of the effective thermal conductivity of colloidal nanosuspensions once optimal values of Kapitza resistance and nanolayer thickness are provided. In perspective, better matching between experimental and predicted values of effective thermal conductivity could be potentially achieved by more accurate measures of Kapitza resistance and nanolayer thickness at the nanoparticle-fluid interface, for example by atomistic simulations or ad hoc experiments.

Acknowledgements

Competing interests

Declarations of interest: none.

References

[1] K.V. Wong, O. De Leon, Applications of nanofluids: current and future, Adv. Mech. Eng. (2010).
[2] H. Sadaf, S. Nadeem, Influences of slip and Cu-blood nanofluid in a physiological study of cilia, Comput. Methods Prog. Biomed. 131 (2016) 169–180.
[3] A. Gizzatov, J. Key, S. Aryal, J. Ananta, A. Cervadoro, A.L. Palange, M. Fasano, C. Stigliano, M. Zhong, D. Di Mascolo, et al., Hierarchically structured magnetic nanoconstructs with enhanced relaxivity and cooperative tumor accumulation, Adv. Funct. Mater. 24 (29) (2014) 4584–4594.
[4] A.M. Hussein, R.A. Bakar, K. Kadirgama, Study of forced convection nanofluid heat transfer in the automotive cooling system, Case Stud. Therm. Eng. 2 (2014) 50–61.
[5] A.V. Azad, N.V. Azad, Application of nanofluids for the optimal design of shell and tube heat exchangers using genetic algorithm, Case Stud. Therm. Eng. 8 (2016) 198–206.
[6] T. Brahim, A. Jemni, Numerical case study of packed sphere wicked heat pipe using Al2O3 and CuO based water nanofluid, Case Stud. Therm. Eng. 8 (2016) 311–321.
[7] A. Andreozzi, O. Manca, S. Nardini, D. Ricci, Forced convection enhancement in channels with transversal ribs and nanofluids, Appl. Therm. Eng. 98 (2016) 1044–1053.
[8] M. Sharifpur, N. Tshimanga, J. Meyer, O. Manca, Experimental investigation and model development for thermal conductivity of α-Al2O3-glycerol nanofluids, Int. Commun. Heat Mass Transf. 85 (2017) 12–22.
[9] M. Amani, P. Amani, A. Kasaeian, O. Mahian, F. Kasaeian, Experimental study on viscosity of spinel-type manganese ferrite nano fluid in attendance of magnetic field, J. Magn. Magn. Mater. 428 (2017) 457–463.
[10] O. Mahian, A. Kianifar, C. Kleinstreuer, M.A. Al-nimr, I. Pop, A.Z. Sahin, A review of entropy generation in nanofluid flow, Int. J. Heat Mass Transf. 65 (2013) 514–532.
[11] S. Rashidi, O. Mahian, E.M. Languri, Applications of nanofluids in condensing and evaporating systems, J. Therm. Anal. Calorim. 131 (3) (2018) 2027–2039.
[12] A. Cardellini, M. Fasano, E. Chiavazzo, P. Asinari, Towards a multiscale simulation approach of nanofluids for volumetric solar receivers: assessing inter-particle potential energy, Energy Procedia 91 (2016) 3–10.
[13] A. Cardellini, M. Fasano, M. Bozorg Bigdeli, E. Chiavazzo, P. Asinari, Thermal transport phenomena in nanoparticle suspensions, J. Phys.: Condens. Matter 28 (48) (2016) 483003.
[14] A. Moradi, E. Sani, M. Simonetti, F. Francini, E. Chiavazzo, P. Asinari, Carbon-nanohorn based nanofluids for a direct absorption solar collector for civil application, J. Nanosci. Nanotechnol. 15 (5) (2015) 3488–3495.
[15] O. Mahian, A. Kianifar, S.A. Kalogirou, I. Pop, S. Wongwises, A review of the applications of nanofluids in solar energy, Int. J. Heat Mass Transf. 57 (2) (2013) 582–594.
[16] J. Subramani, P. Nagarajan, O. Mahian, R. Sathyamurthy, Efficiency and heat transfer improvements in a parabolic trough solar collector using TiO2 nanofluids under turbulent flow regime, Renew. Energy 119 (2018) 19–31.
[17] S.S. Meibodi, A. Kianifar, O. Mahian, S. Wongwises, Second law analysis of a nanofluid-based solar collector using experimental data, J. Therm. Anal. Calorim. 126 (2) (2016) 617–625.
[18] M. Kole, T.K. Dey, Role of interfacial layer and clustering on the effective thermal conductivity of CuO-gear oil nanofluids, Exp. Therm. Fluid Sci. 35 (7) (2011) 1490–1495.
[19] M.B. Bigdeli, M. Fasano, A. Cardellini, E. Chiavazzo, P. Asinari, A review on the heat and mass transfer phenomena in nanofluid coolants with special focus on automotive applications, Renew. Sustain. Energy Rev. 60 (2016) 1615–1633.
[20] M. Amani, P. Amani, A. Kasaeian, O. Mahian, S. Wongwises, Thermal conductivity measurement of spinel-type ferrite MnFe2O4 nano fluids in the presence of a uniform magnetic field, J. Mol. Liq. 230 (2017) 121–128.
[21] C. Kleinstreuer, Y. Feng, Experimental and theoretical studies of nanofluid thermal conductivity enhancement: a review, Nanoscale Res. Lett. 6 (1) (2011) 439.
[22] T.P. Teng, Y.H. Hung, T.C. Teng, H.E. Mo, H.G. Hsu, The effect of alumina/water nanofluid particle size on thermal conductivity, Appl. Therm. Eng. 30 (14–15) (2010) 2213–2218.
[23] M. Fasano, M.B. Bigdeli, Bottom up approach toward prediction of effective thermophysical properties of carbon-based nanofluids, Heat Transf. Eng. (2017) 1–12.
[24] M. Hemmat Esfe, S. Saedodin, M. Bahiraei, D. Toghraie, O. Mahian, S. Wongwises, Thermal conductivity modeling of MgO/EG nanofluids using experimental data and artificial neural network, J. Therm. Anal. Calorim. 118 (2014) 287–294.
[25] M. Hemmat Esfe, S. Saedodin, O. Mahian, S. Wongwises, Thermal conductivity of Al2O3/water nanofluids, J. Therm. Anal. Calorim. 117 (2) (2014) 675–681.

[26] J. Eapen, R. Rusconi, R. Piazza, S. Yip, The Classical Nature of Thermal Conduction in Nanofluids, J. Heat Transf. 132 (10) (2010) 102402.
[27] R. Ruppin, Evaluation of extended Maxwell-Garnett theories, Opt. Commun. 182 (4) (2000) 273–279.
[28] D.A.G. Bruggeman, Berechnung verschiedener physikalischer Konstanten von heterogenen Substanzen. III. Die elastischen Konstanten der quasiisotropen Mischkorper aus isotropen Substanzen, Ann. Phys. 421 (2) (1937) 160–178.
[29] J. Buongiorno, D.C. Venerus, N. Prabhat, T. McKrell, J. Townsend, R. Christianson, Y.V. Tolmachev, P. Keblinski, L.-w. Hu, J.L. Alvarado, et al., A benchmark study on the thermal conductivity of nanofluids, J. Appl. Phys. 106 (9) (2009) 094312.
[30] E. Chiavazzo, M. Fasano, P. Asinari, P. Decuzzi, Scaling behaviour for the water transport in nanoconfined geometries, Nat. Commun. 5 (2014) 4565.
[31] M. Fasano, D. Borri, E. Chiavazzo, P. Asinari, Protocols for atomistic modeling of water uptake into zeolite crystals for thermal storage and other applications, Appl. Therm. Eng. 101 (2016) 762–769.
[32] M. Fasano, D. Borri, A. Cardellini, M. Alberghini, M. Morciano, E. Chiavazzo, P. Asinari, Multiscale simulation approach to heat and mass transfer properties of nanostructured materials for sorption heat storage, Energy Procedia 126 (2017) 509–516.
[33] M.R. Azizian, E. Doroodchi, B. Moghtaderi, The role of liquid layering on the enhancement of thermal conductivity in nanofluids, in: Proceedings of the 14th International Heat Transfer Conference, 2010, pp. 1–7.
[34] K. Raghavan, K. Foster, K. Motakabbir, M. Berkowitz, Structure and dynamics of water at the pt (111) interface: molecular dynamics study, J. Chem. Phys. 94 (3) (1991) 2110–2117.
[35] M. Reedijk, J. Arsic, F. Hollander, S. De Vries, E. Vlieg, Liquid order at the interface of kdp crystals with water: evidence for icelike layers, Phys. Rev. Lett. 90 (6) (2003) 066103.
[36] W. Yu, S.S. Choi, The role of interfacial layers in the enhanced thermal conductivity of nanofluids: a renovated Maxwell model, J. Nanopart. Res. 5 (1) (2003) 167–171.
[37] H. Xie, M. Fujii, X. Zhang, Effect of interfacial nanolayer on the effective thermal conductivity of nanoparticle-fluid mixture, Int. J. Heat Mass Transf. 48 (14) (2005) 2926–2932.
[38] H. Jiang, H. Li, Q. Xu, L. Shi, Effective thermal conductivity of nanofluids considering interfacial nano-shells, Mater. Chem. Phys. 148 (1–2) (2014) 195–200.
[39] A. Kotia, G.K. Ghosh, S.K. Ghosh, Analytical modelling of interfacial thermal conductivity of nanofluids for advanced energy transfer, Iran. J. Sci. Technol. Trans. A: Sci. (2016) 1–9.
[40] R. Pasrija, S. Srivastava, The interfacial layer and the thermal conductivity of nanofluid, Heat Transf. - Asian Res. 43 (3) (2014) 288–296.
[41] D. Alexeev, J. Chen, J.H. Walther, K.P. Giapis, P. Angelikopoulos, P. Koumoutsakos, Kapitza resistance between few-layer graphene and water: liquid layering effects, Nano Lett. 15 (9) (2015) 5744–5749.
[42] B. He, B. Mortazavi, X. Zhuang, T. Rabczuk, Modeling Kapitza resistance of two-phase composite material, Compos. Struct. 152 (2016) 939–946.
[43] A. Ebrahimi, F. Rikhtegar, A. Sabaghan, E. Roohi, Heat transfer and entropy generation in a microchannel with longitudinal vortex generators using nanofluids, Energy 101 (2016) 190–201.
[44] C. Tso, S. Fu, C.Y. Chao, A semi-analytical model for the thermal conductivity of nanofluids and determination of the nanolayer thickness, Int. J. Heat Mass Transf. 70 (2014) 202–214.
[45] E.V. Timofeeva, A.N. Gavrilov, J.M. McCloskey, Y.V. Tolmachev, S. Sprunt, L.M. Lopatina, J.V. Selinger, Thermal conductivity and particle agglomeration in alumina nanofluids: experiment and theory, Phys. Rev. E - Stat. Nonlinear Soft Matter Phys. 76 (6) (2007) 28–39.
[46] A.S. Tascini, J. Armstrong, E. Chiavazzo, M. Fasano, P. Asinari, F. Bresme, Thermal transport across nanoparticle-fluid interfaces: the interplay of interfacial curvature and nanoparticle-fluid interactions, Phys. Chem. Chem. Phys. 19 (4) (2017) 3244–3253.
[47] S.K. Das, N. Putra, P. Thiesen, W. Roetzel, Temperature dependence of thermal conductivity enhancement for nanofluids, J. Heat Transf. 125 (4) (2003) 567.
[48] S. Lee, S.U.-S. Choi, S. Li, J.A. Eastman, Measuring thermal conductivity of fluids containing oxide nanoparticles, J. Heat Transf. 121 (2) (1999) 280.
[49] H.E. Patel, T. Sundararajan, S.K. Das, An experimental investigation into the thermal conductivity enhancement in oxide and metallic nanofluids, J. Nanopart. Res. 12 (3) (2010) 1015–1031.
[50] M.P. Beck, Y. Yuan, P. Warrier, A.S. Teja, The effect of particle size on the thermal conductivity of alumina nanofluids, J. Nanopart. Res. 11 (5) (2009) 1129–1136.
[51] M.P. Beck, Y. Yuan, P. Warrier, A.S. Teja, The thermal conductivity of alumina nanofluids in water, ethylene glycol, and ethylene glycol + water mixtures, J. Nanopart. Res. 12 (4) (2010) 1469–1477.
[52] T. Yiamsawasd, A.S. Dalkilic, S. Wongwises, Measurement of the thermal conductivity of titania and alumina nanofluids, Thermochim. Acta 545 (2012) 48–56.
[53] M. Chandrasekar, S. Suresh, A.C. Bose, Experimental investigations and theoretical determination of thermal conductivity and viscosity of Al2O3/water nanofluid, Exp. Therm. Fluid Sci. 34 (2) (2010) 210–216.
[54] R. Prasher, P. Bhattacharya, P.E. Phelan, Thermal conductivity of nanoscale colloidal solutions (nanofluids), Phys. Rev. Lett. 94 (2) (2005) 025901.
[55] S.H. Kim, S.R. Choi, D. Kim, Thermal conductivity of metal-oxide nanofluids: particle size dependence and effect of laser irradiation, Trans. ASME 129 (2) (2007) 298–307.
[56] G. Xia, H. Jiang, R. Liu, Y. Zhai, Effects of surfactant on the stability and thermal conductivity of Al2O3/de-ionized water nanofluids, Int. J. Therm. Sci. 84 (2014) 118–124.
[57] H.S. Huang, V. Varshney, J.L. Wohlwend, A.K. Roy, Heat transfer at aluminum-water interfaces: effect of surface roughness, J. Nanotechnol. Eng. Med. 3 (3) (2012) 031008.
[58] M. Serebryakova, A. Zaikovskii, S. Sakhapov, D. Smovzh, G. Sukhinin, S. Novopashin, Thermal conductivity of nanofluids based on hollow γ-Al2O3 nanoparticles, and the influence of interfacial thermal resistance, Int. J. Heat Mass Transf. 108 (2017) 1314–1319.
[59] Z. Ge, D.G. Cahill, P.V. Braun, Thermal conductance of hydrophilic and hydrophobic interfaces, Phys. Rev. Lett. 96 (18) (2006) 186101.
[60] S. Diallo, Pore-size dependence and characteristics of water diffusion in slit like micropores, Phys. Rev. E 92 (1) (2015) 012312.
[61] M. Milanese, F. Iacobazzi, G. Colangelo, A. de Risi, An investigation of layering phenomenon at the liquid-solid interface in Cu and CuO based nanofluids, Int. J. Heat Mass Transf. 103 (2016) 564–571.
[62] M. Hu, J.V. Goicochea, B. Michel, D. Poulikakos, Water nanoconfinement induced thermal enhancement at hydrophilic quartz interfaces, Nano Lett. 10 (1) (2009) 279–285.